Numerical analysis of gas exhaust in Wendelstein 7-X using the Direct Simulation Monte Carlo method

***S. Varoutis[1]*, C. Tantos[1], H. Strobel[1], D. Boeyaert[2], Y. Igitkhanov[1], F. Litovoli[1], C. P. Dhard[3], V. Haak[3], D. Naujoks[3] and W7-X Team[3]**

[1]Karlsruhe Institute of Technology, Hermann-von-Helmholtz-Platz 1, 76344, Eggenstein-Leopoldshafen, Germany

[2]Department of Nuclear Engineering and Engineering Physics, University of Wisconsin-Madison, 1500 Engineering Drive, Madison, WI 53706, USA

[2]Max-Planck-Institut für Plasmaphysik, Wendelsteinstraße 1, 17491, Greifswald, Germany

Introduction

Karlsruhe Institute of Technology

- The main objective is that the stellarator concept can meet the requirements of a future fusion reactor by demonstration of high-performance, steady-state operation.
- The improvement of the neutral gas exhaust and the achieved pumping efficiency, which is essential for density control and He exhaust, is the main driver of this analysis.
- A recent numerical study focusing on 2D and 3D W7-X sub-divertor geometries related to the experimental campaign OP 1.2b has been published [1].
- The primary goal of the present study is to extend numerical simulations for <u>Standard magnetic configuration</u>, from low to high-density plasma scenarios and to create a database that correlates exhaust neutral parameters, such as sub-divertor neutral pressure, with upstream plasma parameters like the incoming neutral flux through the pumping gap. This approach aims to better integrate plasma behavior with exhaust optimization, in view of reactor relevant operational conditions.
- The 3D sub-divertor model is related to the OP 2.x in which the “Low-Iota” and “High-Iota” sections are merged into one large volume.
- The DSMC solver of the DIVGAS workflow has been employed.

[1] S. Varoutis et al., Nuclear Fusion, 64, 076011, 2024.

W7-X particle exhaust

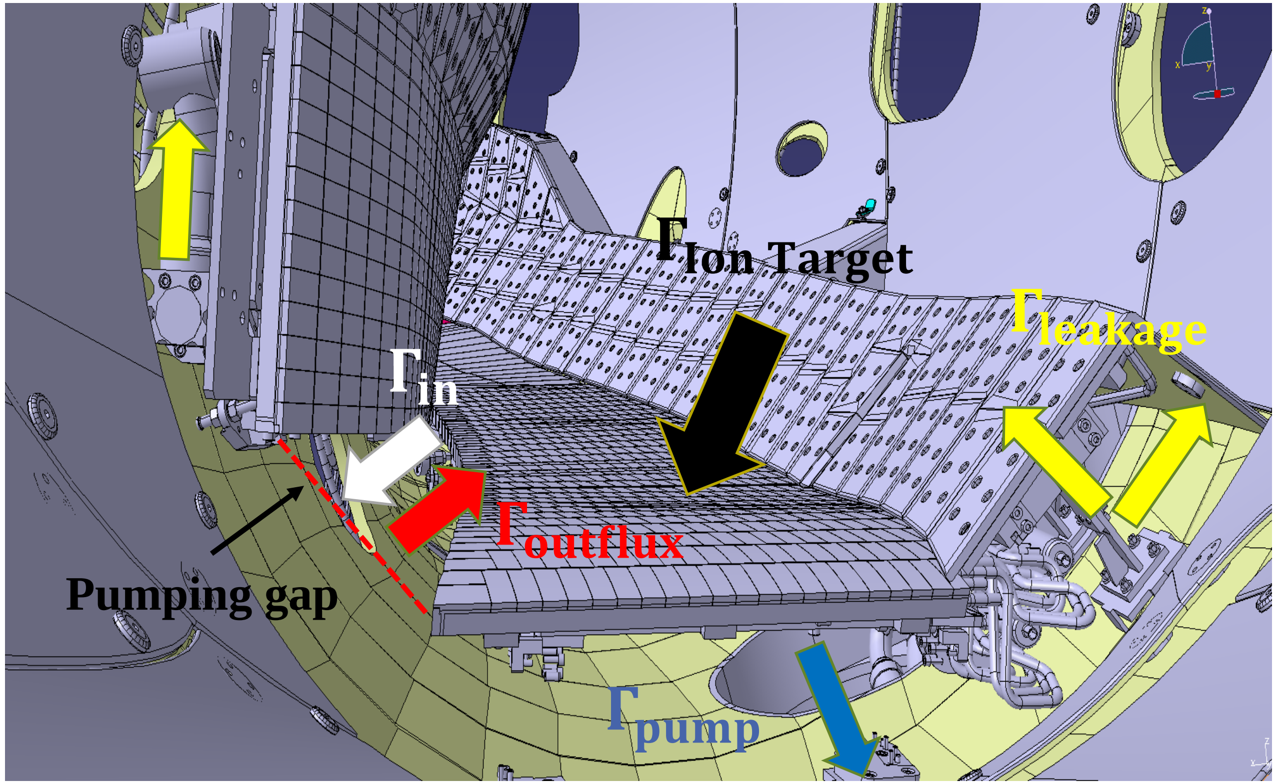

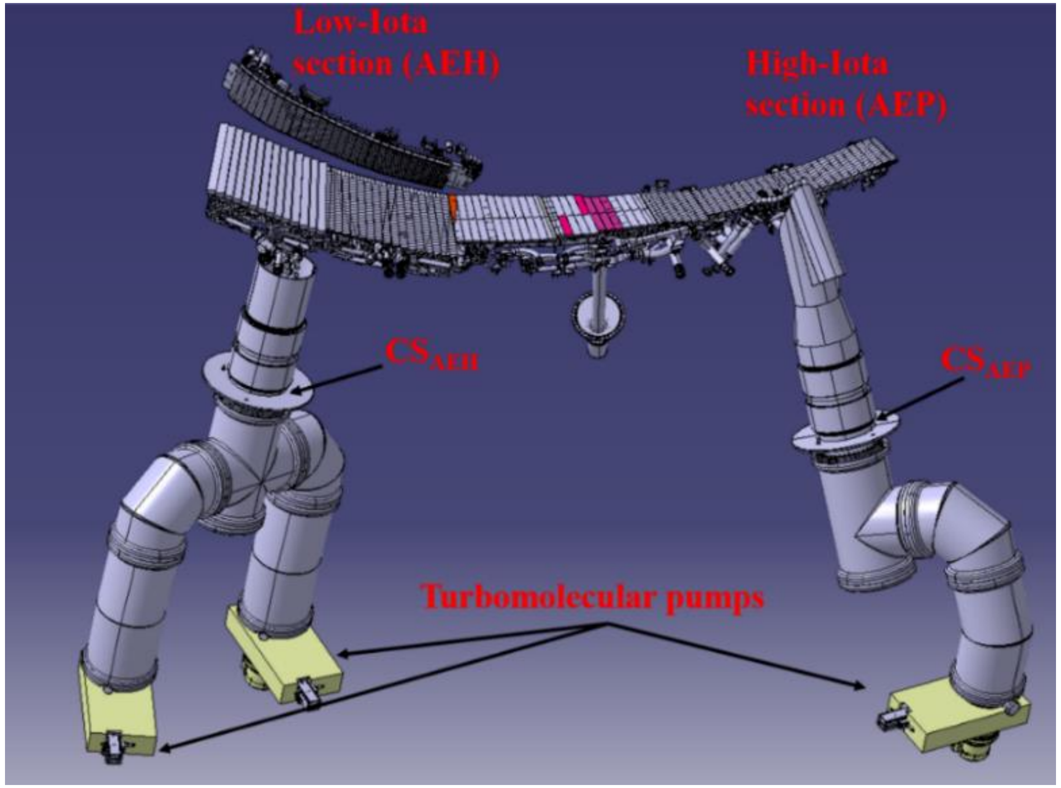

- Gas: H_2, H, T_{in}=0.05 - 4 eV
- $T_{target\ elem.}$= 400 K, T_{vv}=303 K
- Γ_{in} (through pumping gap) = $10^{19} – 10^{24}$ (s^{-1})

- Low-Iota section: 2 TMPs with S_{eff}=3.2 $m^3/s \rightarrow \xi$=0.06 and a cryo-vacuum pump.
- High-Iota section: 1 TMP with S_{eff}=1.46 $m^3/s \rightarrow \xi$=0.0264

W7-X sub-divertor model

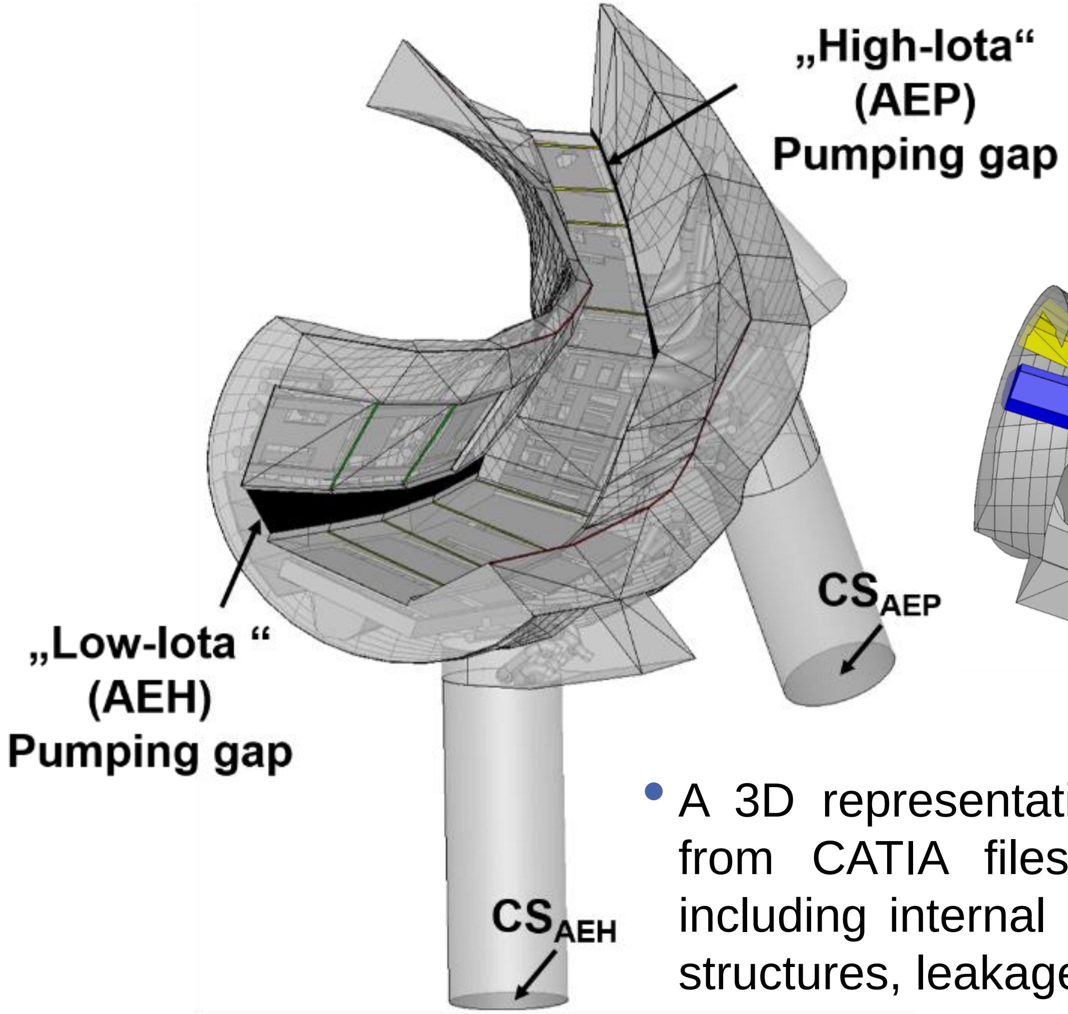

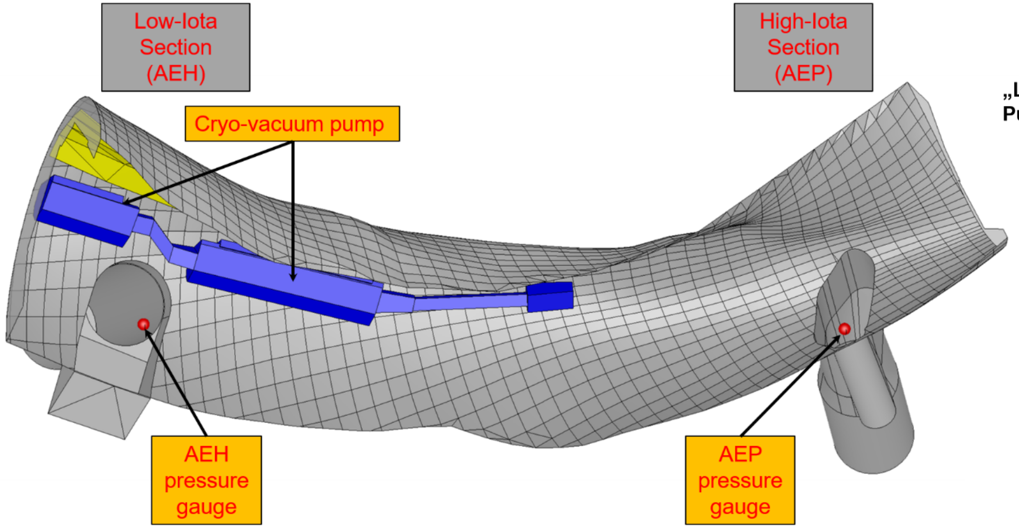

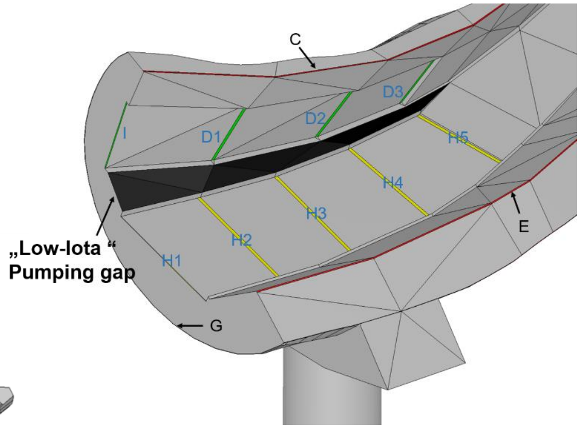

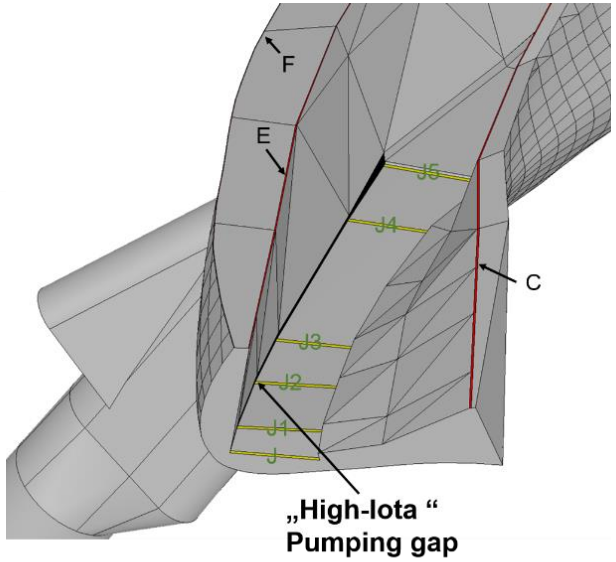

- A 3D representative flow domain has been extracted from CATIA files. A detailed sub-divertor geometry including internal structures (i.e. cooling pipes, support structures, leakages etc) has been considered.

Estimation of the capture coef. for the CVP

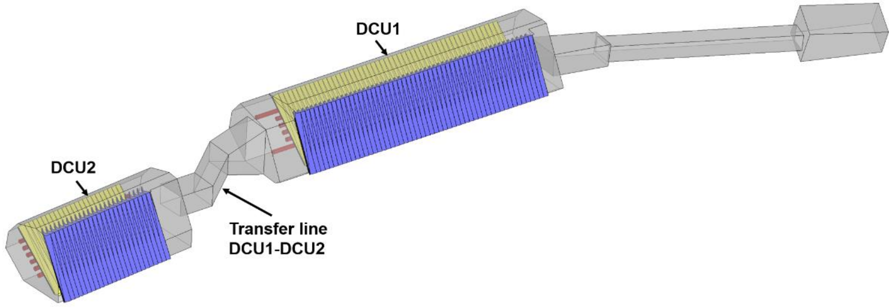

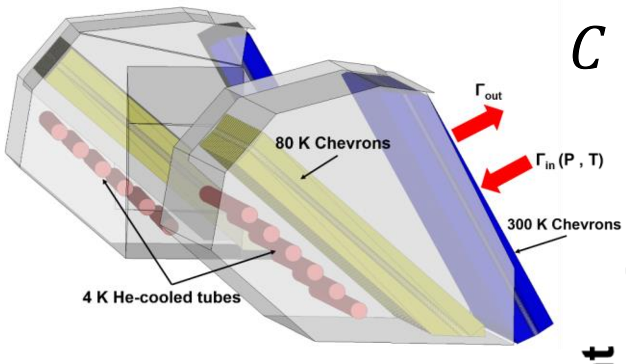

$$C = \Gamma_{pump,He\_tubes}/\Gamma_{in} = 1 - \Gamma_{out}/\Gamma_{in}$$

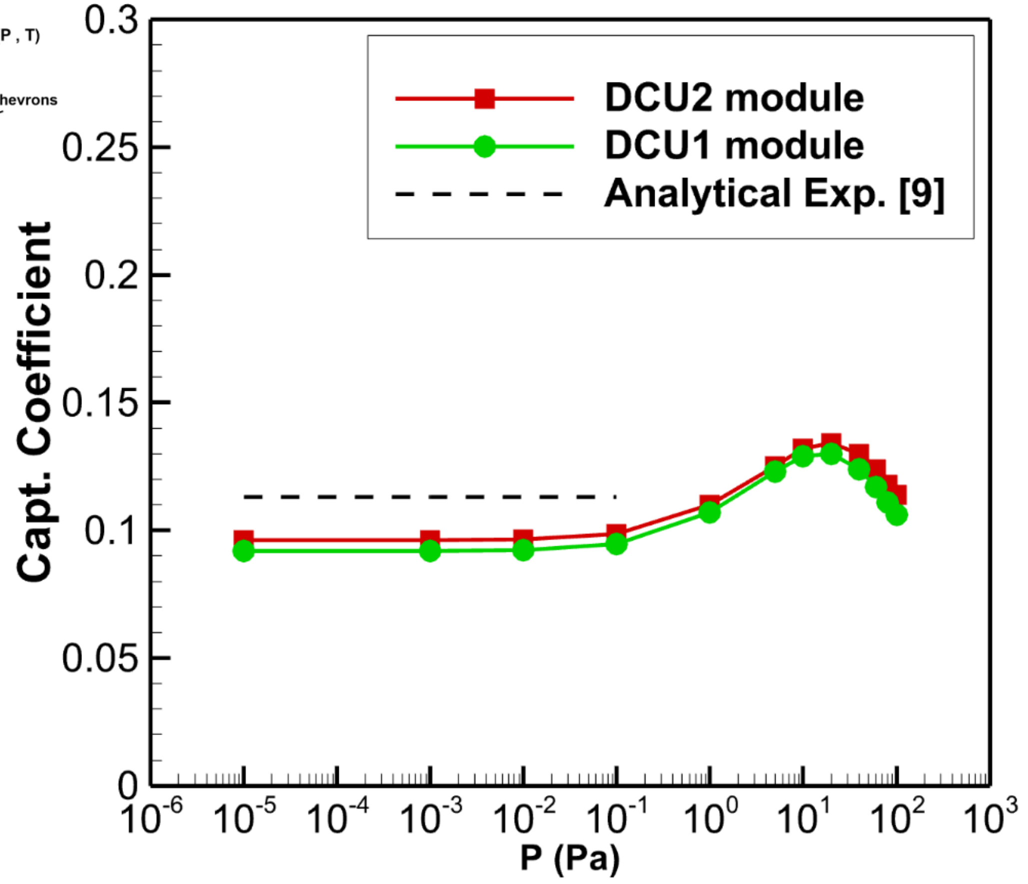

- In the low-pressure range, namely 10^{-5} – 0.1 Pa, the capture coefficient remains constant and is directly linked with the free molecular flow conditions met in this range.
- The relative difference between the DIVGAS simulated values and analytical solutions in the free molecular flow regime equals to ~16%.
- As the pressure in front of the cryo-vacuum pump increases, the capture coefficient also rises, reaching a peak at approximately 10 Pa.
- At higher neutral pressures, the capture coefficient of the CVP decreases, due to choked-flow conditions.

Correlations for P_{div} & Γ_{in}

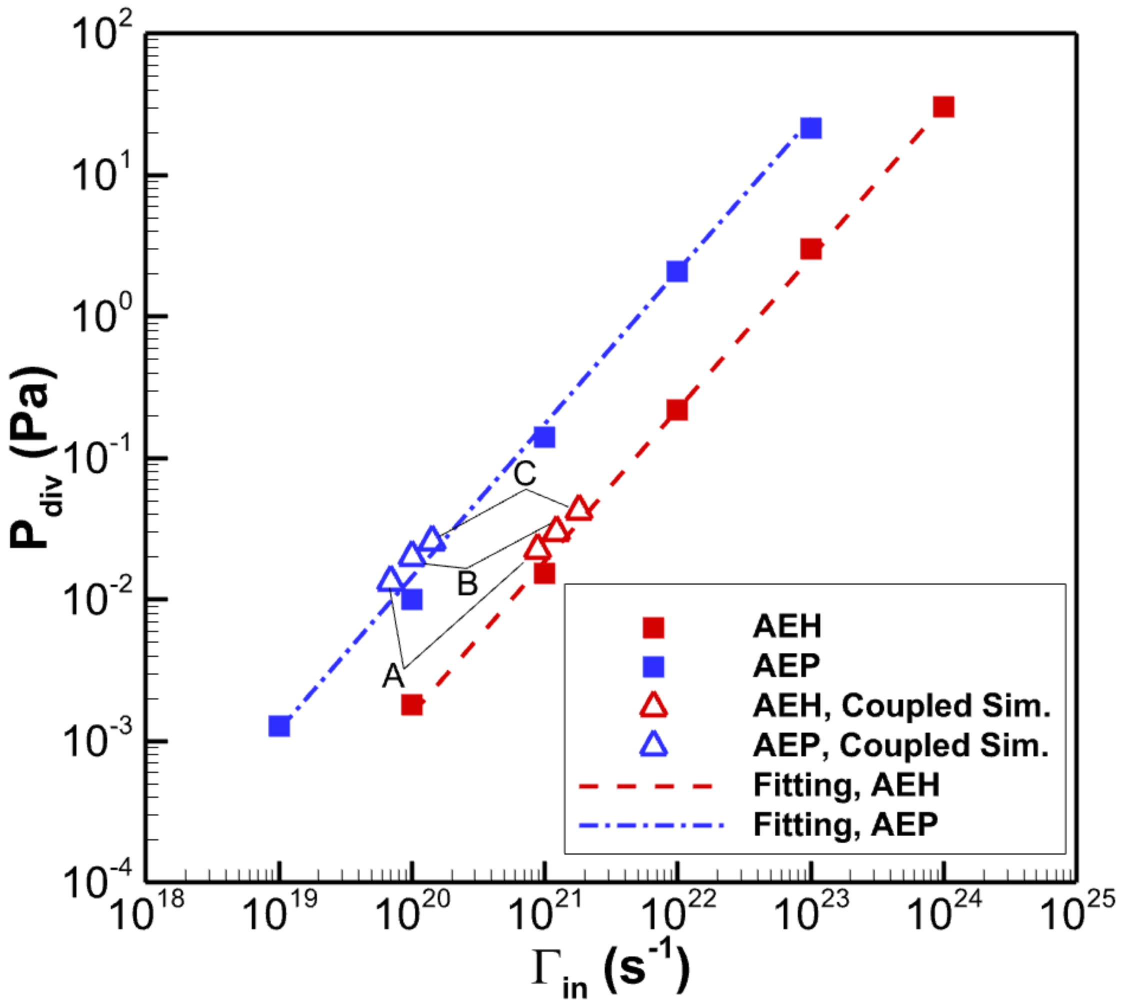

Plasma scenarios:

A. 3 MW of heating power and $n_{e,l.i.}$ = 7x10^{19}, CVP ON, TMP ON
B. 3 MW of heating power and $n_{e,l.i.}$ = 10^{20}, CVP ON, TMP ON
C. 5 MW of heating power and $n_{e,l.i.}$ = 10^{20}, CVP ON, TMP ON

- In log-log scale, the sub-divertor neutral pressure is proportional to the incoming particle flux in both AEH and AEP sections.
- The 3 plasma scenarios lie within the more general scan matrix.
- The correlations which are deduced are:

$$P_{div,AEH} = 5x10^{-25}\Gamma_{in}{}^{1.0747} \qquad R^2 = 0.999$$

$$P_{div,AEP} = 4x10^{-24}\Gamma_{in}{}^{1.0779} \qquad R^2 = 0.998$$

Correlations for P_{div} & $\Gamma_{pump,tot}$

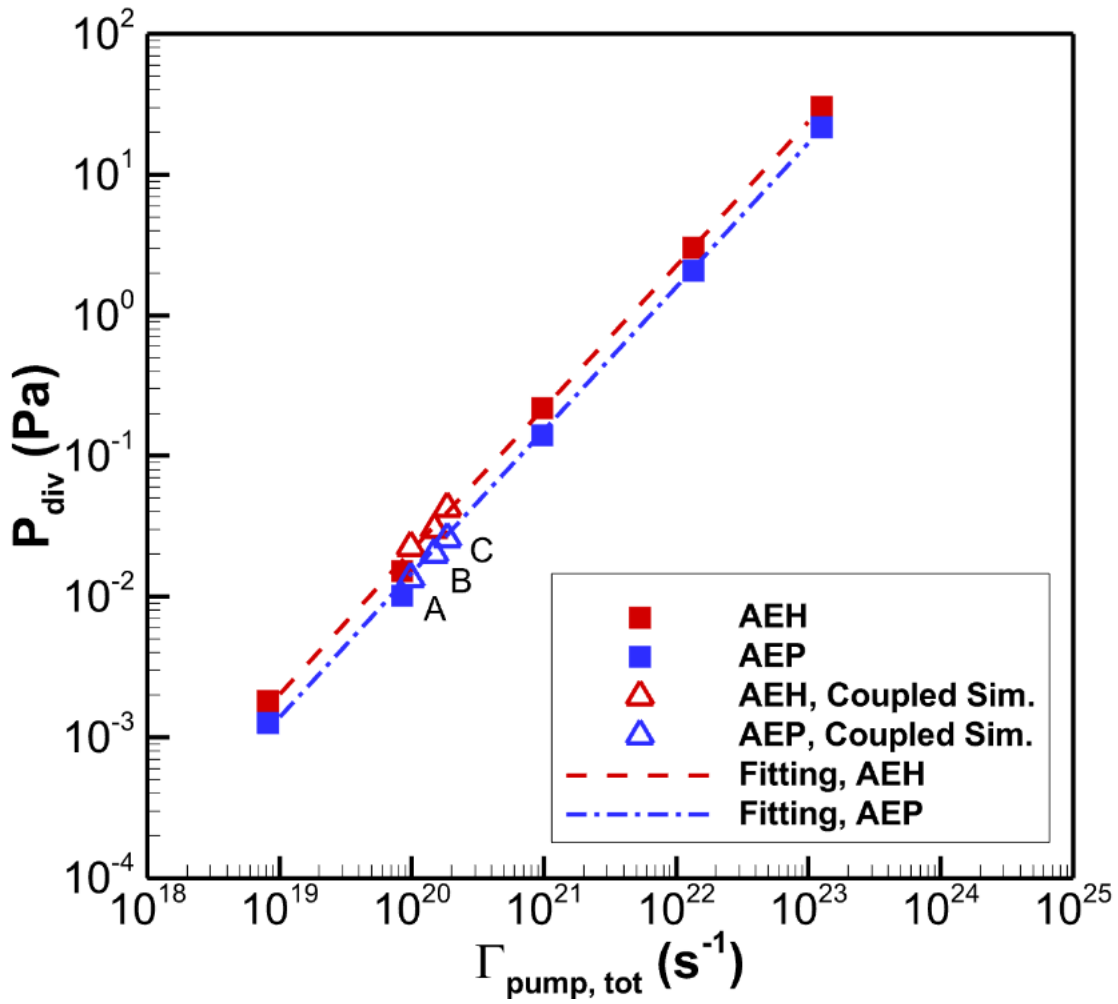

- In log-log scale, the sub-divertor neutral pressure is proportional to the total pumped flux in both AEH and AEP sections, with the effective pumping speed to be a constant of proportionality.
- The estimated effective pumping speed:

$$S_{eff,AEH} = \frac{\Gamma_{pump,tot}}{n_{div,AEH}} \cong 17.2 - 19 \text{ m}^3\text{/s}$$

$$S_{eff,AEP} = \frac{\Gamma_{pump,tot}}{n_{div,AEP}} \cong 24.3 - 28.7 \text{ m}^3\text{/s}$$

- The deduced correlations are:

$$P_{div,AEH} = 10^{-22}\Gamma_{pump,tot}{}^{1.0162} \qquad R^2 = 0.999$$

$$P_{div,AEP} = 6x10^{-23}\Gamma_{pump,tot}{}^{1.0193} \qquad R^2 = 0.998$$

Influence of switching off the CVP

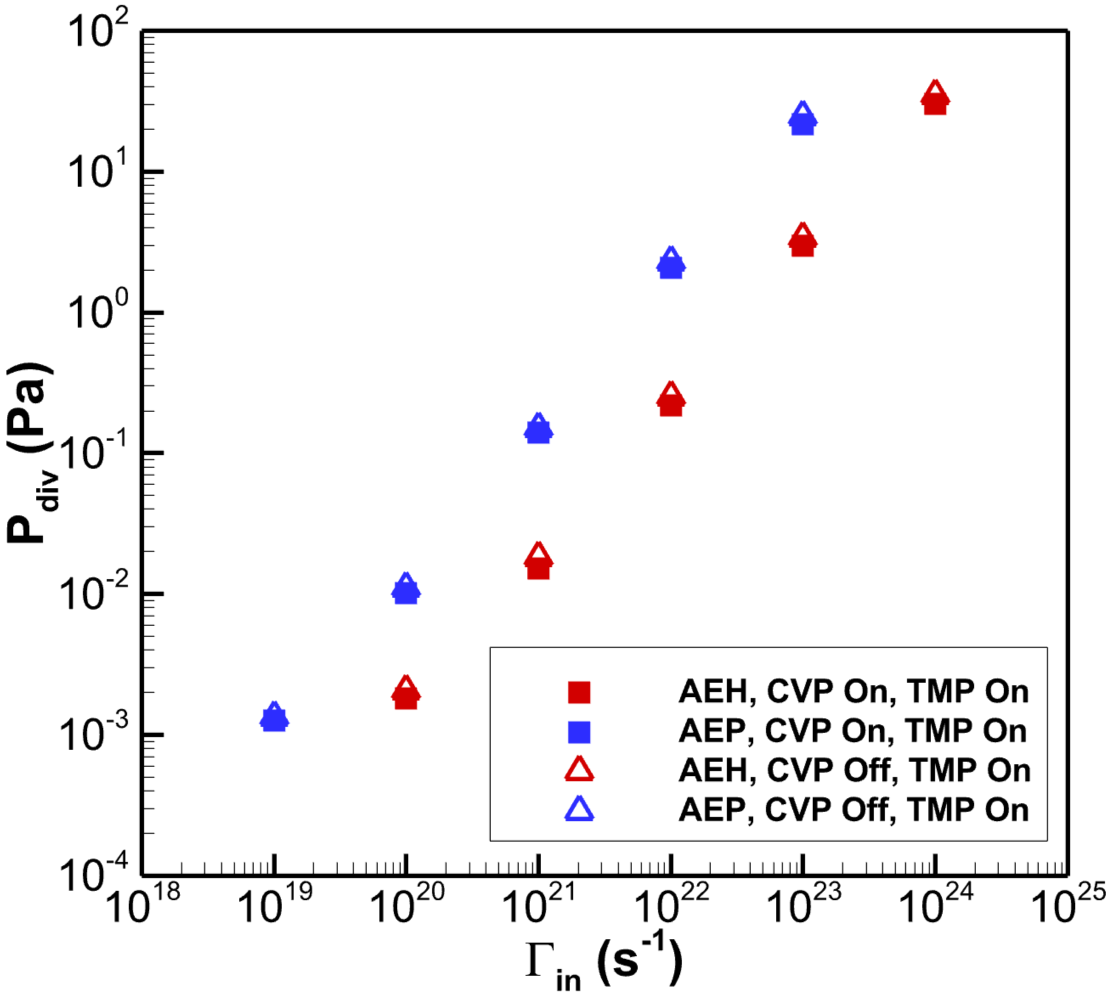

- By switching off the CVP, a pressure increase of ~15% and ~9% in the AEH and AEP sections respectively, is observed.
- The CVP has a moderate effect on the sub-divertor neutral pressure.

Particle balance for plasma scenarios A, B & C

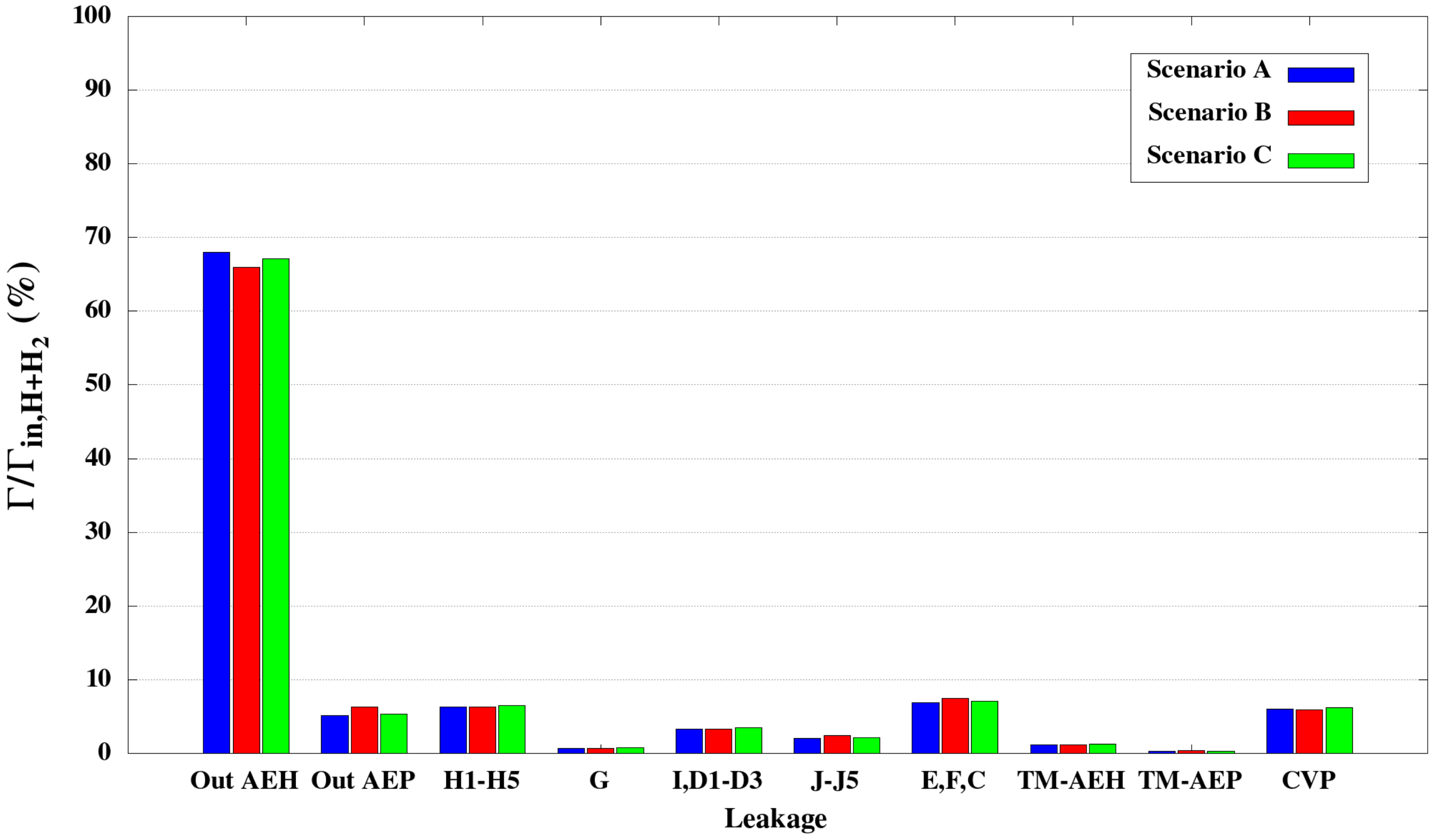

- Scenario C with the highest heating power (i.e 5 MW) is the one, which has a higher pumping efficiency (~8% of the total incoming particle flux).
- Scenario C has the highest total incoming neutral flux to the sub-divertor.
- Through the toroidal as well as the leakages at the horizontal targets, the neutral flux is the highest compared to the other considered leakages.

Estimation of albedo coef. at the pumping gaps

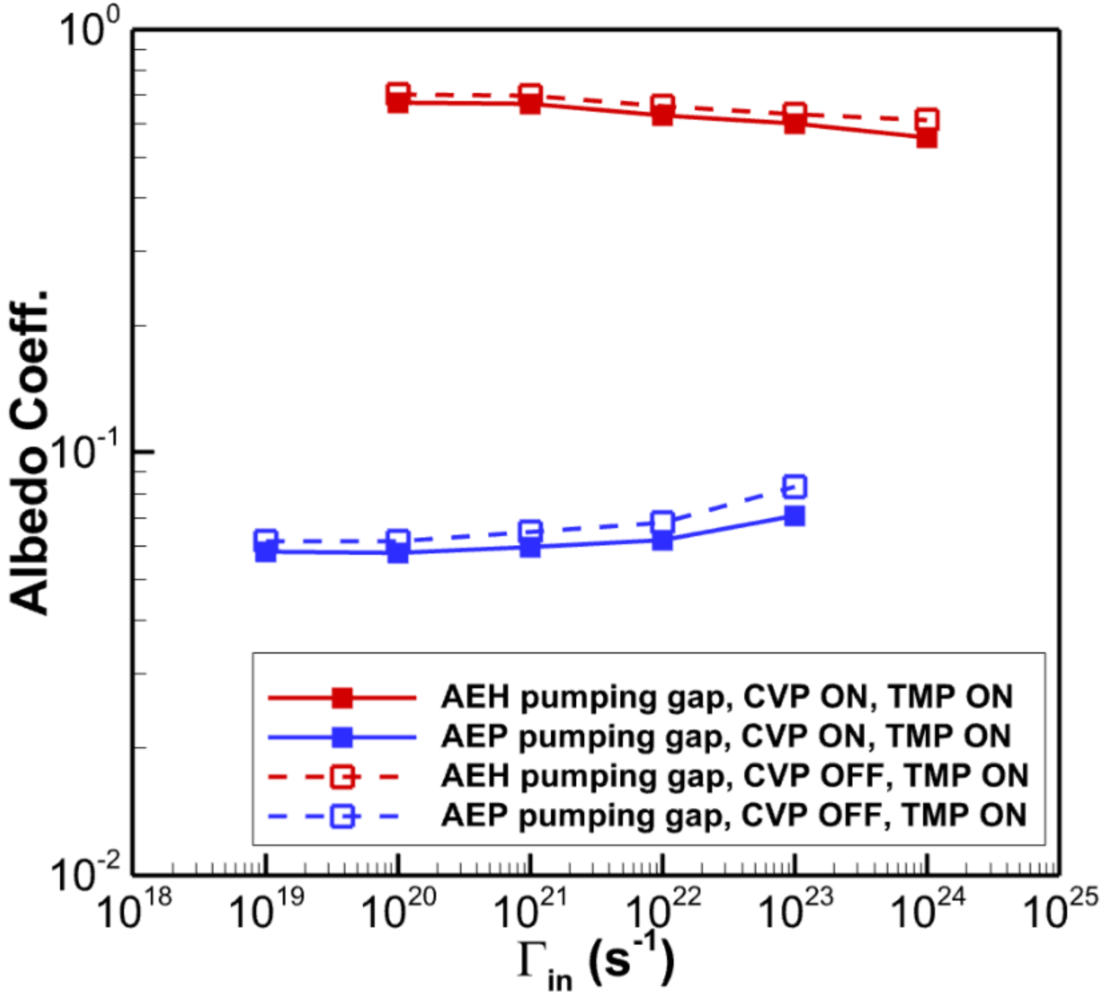

- At the AEH pumping gap, as Γ_{in} increases, the albedo coefficient slightly decreases. This is primarily due to the transition from free molecular flow to viscous flow, which reduces direct reflection from the pumping gap panel.
- Increasing $\Gamma_{in}$by four orders of magnitude results in a 17.3% decrease in the albedo.
- The AEP pumping gap exhibits an increase in the albedo coefficient by approximately 17.8%, attributed to the absence of a pumping gap panel in the AEP section.
- The estimated albedo coefficient can be utilized as an input parameter in future plasma simulations. This approach allows for plasma simulations to account for the sub-divertor geometry, neutral gas dynamics and the corresponding pumping scenario, while reducing the required computational effort.

Conclusions

- The DSMC solver of the DIVGAS workflow has been successfully applied for modelling the 3D neutral gas flow in the W7-X sub-divertor region, for the case of the Standard magnetic configuration and a wide range of incoming neutral particle flux i.e 10^{19} – 10^{24} s^{-1}.
- Three plasma scenarios have been considered, for which is observed that by increasing the heating power, the neutral pressure as well as the resulting pumping efficiency is increased.
- Under steady-state conditions, the sub-divertor neutral pressure is proportional to the incoming neutral particle flux in both AEH and AEP sections, with the effective pumping speed to be a constant of proportionality.
- Such a proportional behavior of the sub-divertor pressure in terms of the incoming neutral flux allows for disentangling the flow conditions in the gas exhaust of W7-X with the upstream plasma parameters.
- The influence of switching off the cryo-vacuum pump on the sub-divertor pressure is rather modest and an increase of the neutral pressure in the AEH and AEP sub-divertor sections by ~15% and ~9% respectively has been estimated.
- Closed-form correlations of the sub-divertor pressure with the total incoming particle flux as well as the total pumped flux at each of the AEH and AEP sections have been proposed.
- The influence of the incoming neutral particle flux on the albedo coefficient at the pumping gaps is relative weak. The albedo database can potentially accelerate future plasma simulations, by replacing the sub-divertor area, while adequately considering all neutral gas dynamics and pumping conditions.

Acknowledgments

- This work has been carried out within the framework of the EUROfusion Consortium, funded by the European Union via the Euratom Research and Training Programme (Grant Agreement No 101052200 — EUROfusion). Views and opinions expressed are however those of the author(s) only and do not necessarily reflect those of the European Union or the European Commission. Neither the European Union nor the European Commission can be held responsible for them.
- The work performed by D. Boeyaert was funded by the U.S. Department of Energy under grant number DE-SC0014210.
- This work was performed within the 6th and 7th cycles of MARCONI-FUSION HPC (project STEL-KIT). Moreover, this research used resources of the National Energy Research Scientific Computing Center, a DOE Office of Science User Facility supported by the Office of Science of the U.S. Department of Energy under Contract No. DE-AC02-05CH11231 using NERSC award FES-ERCAP0028693.
- We acknowledge support by the KIT-Publication Fund of the Karlsruhe Institute of Technology.